

ULTRAHIGH ENERGY NEUTRINOS WITH A MEDITERRANEAN NEUTRINO TELESCOPE

E. Borriello, G. Miele and O. Pisanti

*Dipartimento di Scienze Fisiche, Università di Napoli "Federico II" e INFN Sezione di Napoli,
Complesso Universitario di Monte S. Angelo, Via Cintia, Napoli, 80126, Italy*

ABSTRACT

A study of the ultra high energy neutrino detection performances of a km^3 Neutrino Telescope sitting at the three proposed sites for “ANTARES”, “NEMO” and “NESTOR” in the Mediterranean sea is here performed. The detected charged leptons energy spectra, entangled with their arrival directions, provide an unique tool to both determine the neutrino flux and the neutrino-nucleon cross section.

Neutrinos are one of the main components of the cosmic radiation in the ultra-high energy (UHE) regime. Although their fluxes are uncertain and depend on the production mechanism, their detection can provide information on the sources and origin of the UHE cosmic rays.

From the experimental point of view the detection perspectives are stimulated by the several proposals and R&D projects for Neutrino Telescopes (NT's) in the deep water of the Mediterranean sea, namely **ANTARES** ¹⁾, **NESTOR** ²⁾ and **NEMO** ³⁾, which in the future could lead to the construction of a km^3 telescope as pursued by the **KM3NeT** project ^{4,5)}. Actually, on the **ANTARES** site, a smaller telescope with a surface area of 0.1 km^2 is already under construction ⁶⁾. A further project is **IceCube**, a cubic-kilometer under-ice neutrino detector ^{7,8,9)}, currently being deployed in a location near the geographic South Pole in Antarctica. **IceCube** applies and improves the successful technique of **AMANDA** to a larger volume.

Although NT's were originally thought as ν_μ detectors, their capability as ν_τ detectors has become a hot topic ^{10,11,12,13,14,15,16,17,18)}, in view of the fact that flavor neutrino oscillations lead to nearly equal astrophysical fluxes for the three neutrino flavors. Despite the different behavior of the produced tau leptons with respect to muons in terms of energy loss and decay length, both ν_μ and ν_τ detection are sensitive to the matter distribution near the NT site. Thus, a computation of the event detection rate of a km^3 telescope requires a careful analysis of the surroundings of the proposed site. The importance of the elevation profile of the Earth surface around the detector was already found of some relevance in Ref. ¹⁹⁾, where some of the present authors calculated the aperture of the Pierre Auger Observatory ^{20,21)} for Earth-skimming UHE ν_τ 's. Indeed, air shower experiments can be used as NT's at energies $\gtrsim 10^{18} \text{ eV}$, a topic recently reviewed in ²²⁾. In Ref. ²³⁾ it is estimated the effective aperture for ν_τ and ν_μ detection of a km^3 NT in the Mediterranean

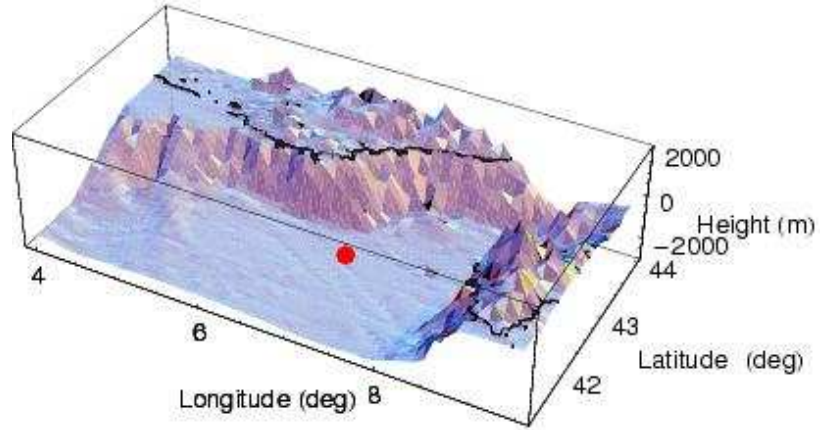


Figure 1: The surface profile of the area near the ANTARES site (red spot) at $42^{\circ} 30' \text{ N}$, $07^{\circ} 00' \text{ E}$. The black curve represents the coast line. The sea plateau depth in the simulation is assumed to be 2685 m. The effective volume starts at an height of 100 m from the seabed, to account for the spacing of the first photomultipliers as foreseen by the current designs.

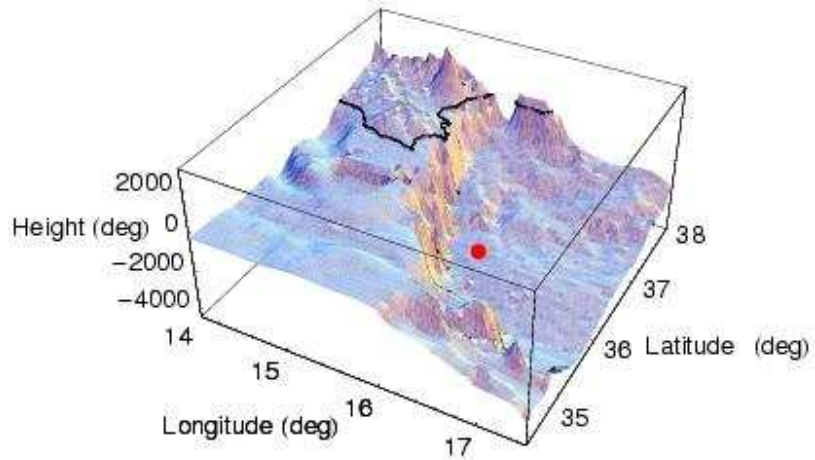


Figure 2: The surface profile of the area near the NEMO site (red spot) at $36^{\circ} 21' \text{ N}$, $16^{\circ} 10' \text{ E}$. The black curve represents the coast line. The sea plateau depth used in the simulation is 3424 m. The effective volume starts at an height of 100 m from the seabed, to account for the spacing of the first photomultipliers as foreseen by the current designs.

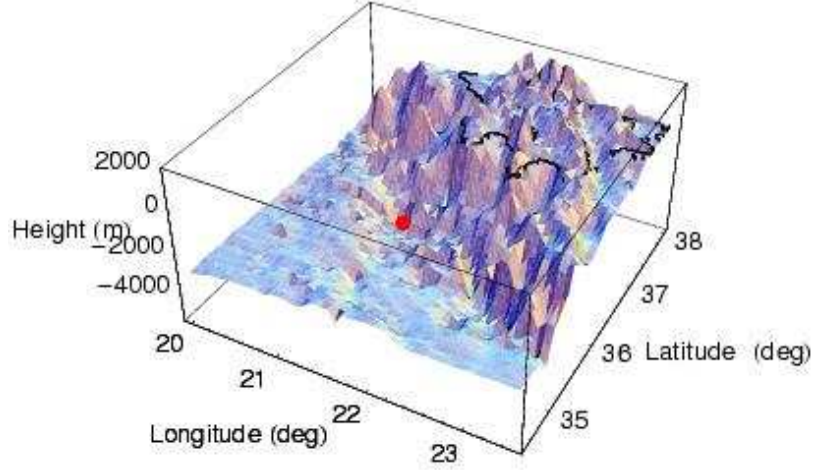


Figure 3: The surface profile of the area near the NESTOR site (red spot) at $36^\circ 21' \text{ N}$, $21^\circ 21' \text{ E}$. The black curve represents the coast line. The sea plateau depth in the simulation is assumed to be 4166 m. The effective volume starts at an height of 100 m from the seabed, to account for the spacing of the first photomultipliers as foreseen by the current designs.

sea placed at any of the three locations proposed by the ANTARES, NEMO and NESTOR collaborations. The characteristics of the three site surface profiles²⁴⁾ are compared by using the DEM of the different areas.

In the present paper we further develop the approach of Ref.²³⁾ in order to apply the detection of UHE ν as a tool to simultaneously measure the UHE neutrino flux and the ν -N cross section in extreme kinematical regions.

Following the formalism developed in²³⁾ we define the km^3 NT *fiducial* volume as that bounded by the six lateral surfaces Σ_a (the subindex $a=\text{D, U, S, N, W, and E}$ labels each surface through its orientation: Down, Up, South, North, West, and East), and indicate with $\Omega_a \equiv (\theta_a, \phi_a)$ the generic direction of a track entering the surface Σ_a . The scheme of the NT fiducial volume and two examples of incoming tracks are shown in Fig. 4. We introduce all relevant quantities with reference to ν_τ events, the case of ν_μ being completely analogous.

Let $d\Phi_\nu/(dE_\nu d\Omega_a)$ be the differential flux of UHE $\nu_\tau + \bar{\nu}_\tau$. The number per unit time of τ leptons emerging from the Earth surface and entering the NT through Σ_a with energy E_τ is given by

$$\left(\frac{dN_\tau}{dt} \right)_a = \int d\Omega_a \int dS_a \int dE_\nu \frac{d\Phi_\nu(E_\nu, \Omega_a)}{dE_\nu d\Omega_a} \int dE_\tau \cos(\theta_a) k_a^\tau(E_\nu, E_\tau; \vec{r}_a, \Omega_a) . \quad (1)$$

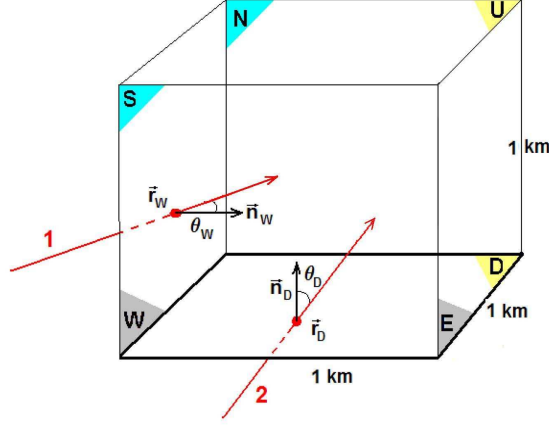


Figure 4: The angle definition and the fiducial volume of a km^3 NT.

The kernel $k_a^\tau(E_\nu, E_\tau; \vec{r}_a, \Omega_a)$ is the probability that an incoming ν_τ crossing the Earth, with energy E_ν and direction Ω_a , produces a τ -lepton which enters the NT fiducial volume through the lateral surface dS_a at the position \vec{r}_a with energy E_τ (see Fig. 4 for the angle definition). If we split the possible events between those with track intersecting the *rock* and the ones only crossing *water*, the kernel $k_a^\tau(E_\nu, E_\tau; \vec{r}_a, \Omega_a)$ is given by the sum of these two mutually exclusive contributions,

$$k_a^\tau(E_\nu, E_\tau; \vec{r}_a, \Omega_a) = k_a^{\tau,r}(E_\nu, E_\tau; \vec{r}_a, \Omega_a) + k_a^{\tau,w}(E_\nu, E_\tau; \vec{r}_a, \Omega_a) . \quad (2)$$

For an isotropic flux we can rewrite Eq. (1), summing over all the surfaces, as

$$\frac{dN_\tau^{(r,w)}}{dt} = \sum_a \int dE_\nu \int dE_\tau \int d\Omega_a \int dS_a \left(\frac{1}{4\pi} \frac{d\Phi_\nu(E_\nu)}{dE_\nu} \right) \cos(\theta_a) k_a^{\tau,(r,w)}(E_\nu, E_\tau; \vec{r}_a, \Omega_a) . \quad (3)$$

By using this expression one can also define the total aperture $A^{\tau(r,w)}(E_\nu)$, with “*r*” and “*w*” denoting the *rock* and *water* kind of events, respectively,

$$\frac{dN_\tau^{(r,w)}}{dt} = \int dE_\nu \left(\frac{1}{4\pi} \frac{d\Phi_\nu(E_\nu)}{dE_\nu} \right) A^{\tau(r,w)}(E_\nu) , \quad (4)$$

where

$$A^{\tau(r,w)}(E_\nu) = \sum_a \int dE_\tau \int d\Omega_a \int dS_a \cos(\theta_a) k_a^{\tau,(r,w)}(E_\nu, E_\tau; \vec{r}_a, \Omega_a) . \quad (5)$$

Of course, the same quantities can be defined for muons coming from the charged-current interactions of ν_μ .

In Fig. 5 we compare the detection performances of a km^3 NT placed at one of the three sites in the Mediterranean sea. The **NESTOR** site shows the highest values of the

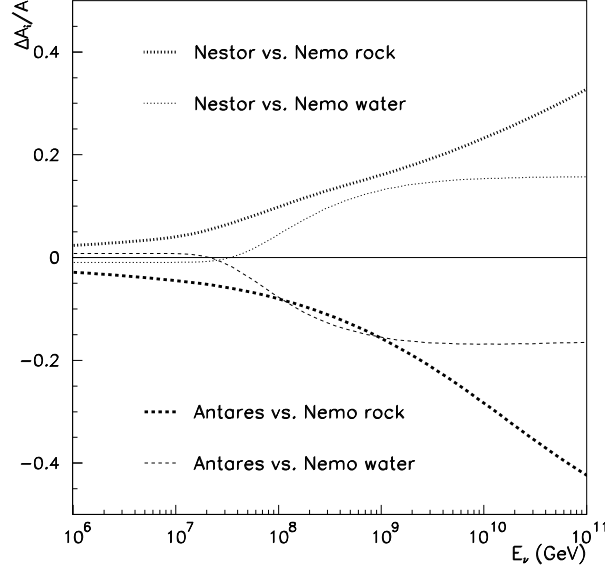


Figure 5: A comparison of the effective apertures $A^{\tau((r,w))}(E_\nu)$ for the three NT sites. We plot the ratios $[A^{\tau((r,w))}(\text{NESTOR}) - A^{\tau((r,w))}(\text{NEMO})]/A^{\tau((r,w))}(\text{NEMO})$ and $[A^{\tau((r,w))}(\text{ANTARES}) - A^{\tau((r,w))}(\text{NEMO})]/A^{\tau((r,w))}(\text{NEMO})$ versus the neutrino energy.

τ -aperture for both *rock* and *water*, due to its larger depth and the particular matter distribution of the surrounding area, while the lowest rates are obtained for **ANTARES**. The aperture in the three sites can be quite different at high energy but, in order to get the expected number of UHE events per year, one has to convolve the aperture with a neutrino flux which typically drops rapidly with the energy. Although the percentage value of the matter effects remains unchanged, in this very low statistics regime they can be hardly distinguished; still, they can be enhanced by an appropriate choice of the detector shape.

Knowing the aperture of the NT at each site, we can compute the expected τ event rate, once a neutrino flux is specified. In Table 1 these rates are shown assuming a

Surf.	ANTARES	NEMO	NESTOR
D	0.0059/0	0.0059/0	0.0058/0
U	0/0.1677	0.0002/0.2133	0.0002/0.2543
S	0.0185/0.1602	0.0256/0.1773	0.0240/0.2011
N	0.0241/0.1540	0.0229/0.1823	0.0321/0.1924
W	0.0212/0.1584	0.0335/0.1691	0.0265/0.2002
E	0.0206/0.1589	0.0190/0.1875	0.0348/0.1907
Total	0.090/0.799	0.107/0.929	0.123/1.039

Table 1: Estimated rate per year of *rock/water* τ events at the three km^3 NT sites for a GZK-WB flux^{(23), (25)}. The contribution of each detector surface to the total number of events is also reported.

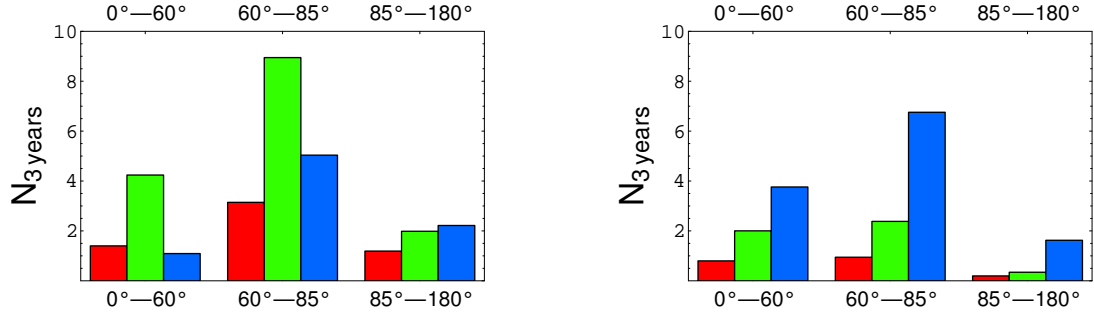


Figure 6: In the two panels are reported the number of events ($\mu + \tau$) collected in three years from a km^3 NT. The left panel concerns the events with energy lost in the detector in the range 10^5 - 10^8 GeV, whereas on the right the events have an energy deposited larger than 10^8 GeV. See the text for further details.

GZK-WB flux^{25,23)}. The effect due to the local matter distribution is responsible for the N-S, W-E and NE-SW asymmetries for the **ANTARES**, **NEMO** and **NESTOR** sites, respectively, as expected from the matter profiles shown in Figs. 1, 2 and 3. These matter effects, for the specific UHE flux considered (GZK-WB), correspond to an enhancement of *rock* events which goes from 20 to 50% for the three sites, respectively, and a screening factor for *water* events from 3 to 10%. The largest relative difference among lateral surfaces is in the case of W/E for **NEMO**, where the huge wall to the west of the site (see Fig. 2) improves the rate by about 75%, almost a factor 2! Notice also that the *water* events from the U surface are basically proportional to the depth.

Due to the dependence of Eq. (3) on the neutrino flux and the different behavior of $k_a^{\tau,r}(E_\nu, E_\tau; \vec{r}_a, \Omega_a)$ and $k_a^{\tau,w}(E_\nu, E_\tau; \vec{r}_a, \Omega_a)$ as functions of the neutrino-nucleon cross section, $\sigma_{CC}^{\nu N}$, one can imagine to use the detected events, properly binned for energy loss and arrival direction, in order to obtain information on both the neutrino flux and the neutrino-nucleon cross section. In particular, since the real observable is the energy deposited in the detector and not the energy and/or the nature of the charged lepton, either μ or τ , crossing the NT, one must sum the two contributions. In fact, the events whose topology allows for determining the nature of the charged lepton are a negligible fraction of the expected total number.

In the two panels of Figure 6 are reported the number of events ($\mu + \tau$) collected in three years from a km^3 NT. In particular the left panel concerns the events where the energy deposited in the detector is in the range 10^5 - 10^8 GeV, whereas the one on the right reports events where the energy lost is larger than 10^8 GeV. For each panel the events have been split in three bins according to their arrival directions (0° represents the vertical downgoing direction). Fixing the panel and the arrival direction range, the three bars of the histogram represents three different neutrino fluxes and $\sigma_{CC}^{\nu N}$ chosen. In particular from left to right we have the GZK-WB^{23),24)} flux and standard cross section, the GZK-WB^{23),24)} flux and three times the standard cross section and finally, the more copious GZK-H^{23),24)} flux and standard cross section. Note that

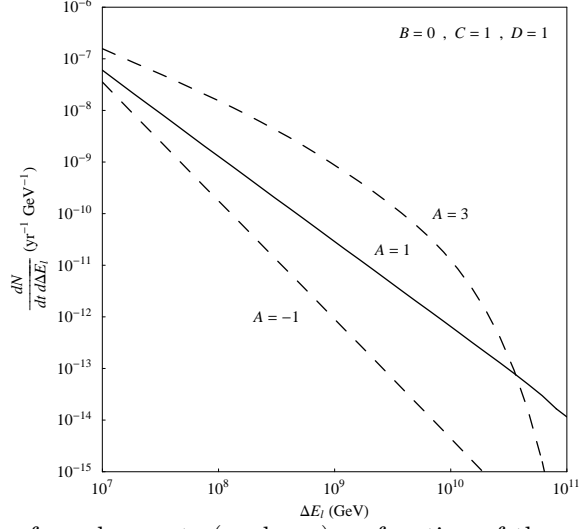


Figure 7: The number density of yearly events (μ plus τ) as function of the energy deposited by the charged lepton ΔE_l for different values of A and with $B = 0$ and $C = D = 1$. The solid line represent the standard scenario.

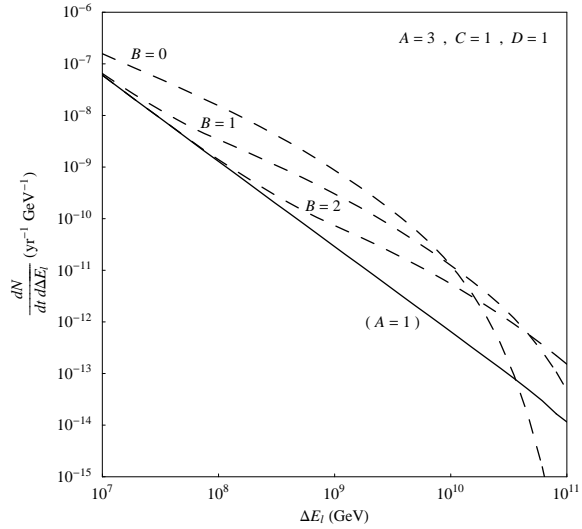


Figure 8: The number density of yearly events (μ plus τ) as function of the energy deposited by the charged lepton ΔE_l for different values of B and with $A = 3$ and $C = D = 1$. The solid line represent the standard scenario.

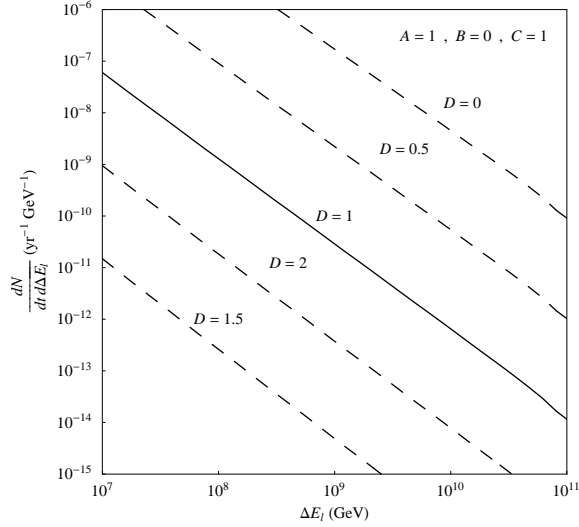


Figure 9: The number density of yearly events (μ plus τ) as function of the energy deposited by the charged lepton ΔE_l for different values of D and with $A = C = 1$ and $B = 0$. The solid line represent the standard scenario.

the total number of events for GZK-WB with $3\sigma_{CC}^{\nu N}$ and for GZK-H with standard cross section are the same. The different flux/cross section configurations can be disentangled by observing the different behavior of the height of the bars as function of the energy lost and arrival direction.

In order to study the sensitivity to both neutrino flux and $\sigma_{CC}^{\nu N}$ it is necessary to parameterize their standard expression and the possible departure from it. In particular by using a standard Waxman-Bahcall ¹³⁾ ($C=D=1$) as a conservative reference for the neutrino flux we allow for a variation of its steepness via the exponent D and for the normalization through the multiplicative factor C , namely:

$$\phi_{WB} \cong 1.3 \cdot 10^{-8} C \epsilon_\nu^{-2D} \text{GeV}^{-1} \text{cm}^{-2} \text{s}^{-1} \text{sr}^{-1} . \quad (6)$$

In the same way, for the neutrino-nucleon cross section one can parameterize the presence of new physics by assuming a departure from the standard expression ²⁶⁾ in terms of two free parameters, A and B , whose standard values are $A = 1$ and $B = 0$:

$$\sigma_{CC}^{\nu N} = 10^{-36} \text{cm}^2 \begin{cases} 0.677 \epsilon_\nu^{0.492} ; & 2.00 \cdot 10^4 < \epsilon_\nu < 1.20 \cdot 10^7 \\ 5.54 \epsilon_\nu^{0.363} ; & 1.20 \cdot 10^7 < \epsilon_\nu < 1.20 \cdot 10^{7+B} \\ 5.54 \cdot 10^{0.363(1-A)(7.08+B)} \epsilon_\nu^{0.363A} ; & 1.20 \cdot 10^{7+B} < \epsilon_\nu \end{cases} \quad (7)$$

where $\epsilon_\nu \equiv E_\nu/\text{GeV}$. In particular B fixes the energy value where new physics appears and A is the change in the energy slope of $\sigma_{CC}^{\nu N}$. In Figures 7, 8 and 9 it is reported the effect of the variation of the single parameter A , B , D on the number density of

yearly events (μ plus τ) as a function of the energy deposited by the charged lepton ΔE_l . The factor C has been fixed to its standard value ($C = 1$) since it is just a normalization and thus simply correlated to the exposure time needed to achieve the proper event statistics.

The quite relevant effect shown by Figures 7, 8 and 9 supports once more the idea that a km^3 NT can provide a real chance to both measure UHE neutrino flux and the neutrino-nucleon cross section in the extreme kinematical region, where some new physics could appear. Of course the real feasibility of such measurements will crucially depend of the size of the neutrino flux which fixes the time required to reach a reasonable statistics. Then, while in this exercise we adopted an extreme conservative point of view working with Waxman-Bahcall like fluxes, one can wish for a more optimistic real situation.

1. References

- 1) Aslanides E et al., 1999 “A Deep Sea Telescope for High Energy Neutrinos, Proposal,” astro-ph/ 9907432.
- 2) Bottai S, 1999 Contribution to 26th ICRC, Salt Lake City, AIP Conf. Proc. **516** vol 2 456.
- 3) Riccobene G, 2002 Proc. of the Workshop on Methodical Aspects of Underwater/Ice Neutrino Telescopes, 61
- 4) Katz U F, “Neutrino telescoping in the Mediterranean sea,” 2006 *Prog. Part. Nucl. Phys.* **57** 273.
- 5) Katz U F, “KM3NeT: Towards a km^3 Mediterranean neutrino telescope,” 2006 [astro-ph/0606068].
- 6) J. A. Aguilar *et al.* [ANTARES Collaboration], “First results of the instrumentation line for the deep-sea ANTARES neutrino telescope,” *Astropart. Phys.* **26** (2006) 314 [astro-ph/0606229].
- 7) Ahrens J et al., 2000 *The IceCube NSF Proposal*.
- 8) Ahrens J et al., 2001 *IceCube Conceptual Design Document*.
- 9) Ahrens J et al., “Sensitivity of the IceCube detector to astrophysical sources of high energy muon neutrinos,” 2004 *Astropart. Phys.* **20** 507.
- 10) R. Gandhi, C. Quigg, M. H. Reno and I. Sarcevic, “Ultrahigh-Energy Neutrino Interactions,” *Astropart. Phys.* **5** (1996) 81 [hep-ph/9512364].
- 11) Dutta S I, Reno M H and Sarcevic I, 2000 “Tau-neutrinos underground: Signals of $\nu/\mu \rightarrow \nu/\tau$ oscillations with extragalactic neutrinos,” *Phys. Rev. D* **62** 123001.
- 12) González-García M C, Halzen F and Maltoni M, “Physics reach of high-energy and high-statistics Icecube atmospheric neutrino data,” 2005 *Phys. Rev. D* **71** 093010.

- 13) Anchordoqui L and Halzen F, "Icehep High Energy Physics At The South Pole," 2005 [hep-ph/0510389].
- 14) Yoshida S, Ishibashi R and Miyamoto H, "Propagation of extremely-high energy leptons in the earth: Implications to their detection by the IceCube neutrino telescope," 2004 *Phys. Rev. D* **69** 103004.
- 15) Beacom J F et al., "Measuring flavor ratios of high-energy astrophysical neutrinos," *Phys. Rev. D* **68**, 093005 (2003) [Erratum-ibid. *D* **72**, 019901 (2005)].
- 16) Athar H, Parente G and Zas E, "Prospects for observations of high-energy cosmic tau-neutrinos," *Phys. Rev. D* **62**, 093010 (2000).
- 17) Bugaev E, Montaruli T, Shlepin Y and Sokalski I, "Propagation of tau neutrinos and tau leptons through the earth and their detection in underwater / ice neutrino telescopes," *Astropart. Phys.* **21**, 491 (2004).
- 18) Ishihara A (IceCube Collaboration), 2006 *IceCube projects and its EHE physics capability*, Proceedings of CRIS06, Catania (Italy), to appear in *Nucl. Phys. Proc. Suppl.*
- 19) Miele G, Pastor S and Pisanti O, "The aperture for UHE tau neutrinos of the Auger fluorescence detector using a digital elevation map," 2006 *Phys. Lett. B* **634** 137.
- 20) Pierre Auger Collaboration, 1996 *The Pierre Auger Project Design Report*, FERMILAB-PUB-96-024.
- 21) Abraham J et al. (Pierre Auger Collaboration), "Properties and performance of the prototype instrument for the Pierre Auger Observatory," 2004 *Nucl. Instrum. Meth. A* **523** 50.
- 22) Zas E, "Neutrino detection with inclined air showers," 2005 *New J. Phys.* **7** 130.
- 23) A. Cuoco, G. Mangano, G. Miele, S. Pastor, L. Perrone, O. Pisanti and P. D. Serpico, *JCAP* **0702**, 007 (2007) [arXiv:astro-ph/0609241].
- 24) U.S. Department of Commerce, National Oceanic and Atmospheric Administration, National Geophysical Data Center, 2001 *2-minute Gridded Global Relief Data (ETOPO2)*, <http://www.ngdc.noaa.gov/mgg/fliers/01mgg04.html>
- 25) Waxman E and Bahcall J N, "High energy neutrinos from astrophysical sources: An upper bound," 1999 *Phys. Rev. D* **59** 023002.
- 26) Gandhi R et al., "Neutrino interactions at ultrahigh energies," *Phys. Rev. D* **58**, 093009 (1998).